Validation of Permeability and Relative Permeability Data Using Mercury Injection Capillary Pressure Data

Rasoul Arabjamaloei[1], *David Daniels*[2], *Einar Ebeltoft*[3], *Egil Petersen*[3], *Richard John Pitman*[3], *Douglas Ruth*[1,*]

[1]University of Manituba
[2]Equinor Canada Ltd.
[3] Equinor ASA, Norway.

Abstract. This paper reports on a study with the objective to validate a set of core analysis data using a combination of mercury injection capillary pressure (MICP) data and statistical correlation techniques. The data set is from an off-shore reservoir in Atlantic Canada. Analysis of this reservoir was complicated by the fact that the permeabilities of the samples were high, greater than 2400 mD. The analysis was done using an existing data set, not a data set specifically tailored for the techniques used in the analysis. The data analyzed included samples that represented seven zones in a single well. Porosities and permeabilities were available for the MICP samples. Electrical properties, along with porosities and permeabilities, were available on samples from each zone, but not from the same depths as the MICP samples. Steady-state relative permeabilities (SSRP) were available for stacked samples in each zone; one of the samples in the stack was a companion sample for one of the MICP samples from that zone. The MICP results were used to validate the permeability measurements using both the Swanson method (SM) and the Ruth-Lindsay-Allen (RLAM) method. The SM, using published correlation parameters, significantly under-predicted the permeabilities; the RLAM, which uses no correlation parameters, gave predictions within a maximum error of just over 33% and a mean error of -12%. The MICP data was used to validate the shapes of the SSRP curves using the Gates and Tempelaar-Lietz method (GT-LM), the Burdine method (BM), and a modified Burdine method (MBM). The GT-LM, which uses no correlation parameters, provided good predictions of the wetting phase SSRP curves but very poor predictions of the non-wetting phase SSRP curves. The BM, using published correlation parameters, provided poor predictions of the wetting phase SSRP curves but improved predictions of the non-wetting phase SSRP curves. The MBM provided good predictions of the wetting phase SSRP curves and acceptable predictions of the non-wetting phase SSRP curves. The MBM method does use a correlation parameter but a single value was used for all seven zones. This work provides a protocol for validating core analysis data that can be implemented in a straightforward manner to determine the "quality" of the data. The results emphasize the importance of MICP as an experimental technique. A proposed modified workflow is presented that would optimize the validation protocol.

1 Introduction

Whenever core analysis data is reviewed, the question of data validity must be addressed. Data validation is a two part process. The first question that must be asked is: Are the values what are expected? This question rests on the implicit assumption that we can actually state what we expect. Even with the most sophisticated imaging and flow simulation, there is still great uncertainty in predicting transport phenomena, particular multi-component flow phenomena, in porous media based on primary information such as pore images and fluid properties. If it is determined that the transport properties are sensible, then the data can be considered to be validated. However, if the data does not agree with expectations, then a further question must be asked: Is the data correct? The "correctness" of the data refers to the accuracy and precision of the experiment itself. Unlike many fields of testing, except for synthetic samples such as those made by sintering glass, porous samples with well documented properties are not readily available. However, careful examination of laboratory procedures and close scrutiny of data analysis techniques will generally determine if the data is "correct". If the data is judged to be "correct" and the results do not conform to expectations, then sources of the anomalies can be explored with confidence. The present study was conducted to determine if a relatively straightforward protocol can be used to validate a set of data for a well from off-shore

* Corresponding author: Douglas.Ruth@umanitoba.ca

Atlantic Canada. Rather than use sophisticated core images and predictive techniques, the protocol relies on determining if data from a number of different core analysis tests can be rationalized without the use of a large number of correlation ("fitting") parameters. The present validation process relies on the availability of mercury injection capillary pressure curves.The protocol was tested on an existing data not one specifically tailors for this study.

2 Permeability Validation

The foundational data for this study were mercury injection capillary pressure (MICP) results for a suite of seven samples. The properties of these samples are shown in Table 1. The first row in this table shows the Klinkenberg corrected permeabilities. The last row in this table are the permeabilities calculated by the service laboratory from the MICP data using the Swanson method [1]. All of the samples have high permeabilities, ranging from just over 2000 mD to just under 8000 mD. The first stage in validating the data was to determine if the MICP results could be used to accurately predict the sample permeability. This was done in three different ways: using a simple permeability-porosity cross plot; using the Swanson method (SM) [1]; and using the Ruth-Lindsay-Allen method (RLAM) [2].

Table 1. Basic Data for the MICP Samples

Sample Number	#7	#18	#25	#36	#43	#48	#53
Klinkenberg Corrected Permeability (*mD*)	2407	6317	6854	3565	5810	7855	6540
Helium Porosity	0.286	0.316	0.259	0.291	0.305	0.296	0.262
Helium Pore Volume (*cc*)	0.947	0.833	0.754	0.940	0.698	1.174	0.705
Bulk Volume (*cc*)	3.313	2.635	2.914	3.234	2.290	3.965	2.694
Grain Volume (*cc*)	2.366	1.802	2.161	2.294	1.592	2.791	1.989
MICP Permeability (*mD*)	1046	2686	2020	1283	2094	2587	1125

Figure 1 shows the permeability-porosity cross plot along with the best fit regression line. Clearly, there is no evident trend in this data. Both the SM and the RLAM rely on interpreting the MICP curves to obtain a representative pore (tube) diameter on which to base the permeability prediction. Figure 2 shows the pressure versus vacuum saturation for the seven curves. The interpretation of these curves used values of interfacial tension and contact angle of 0.480 N/m and 140° respectively. All of the MICP data appear to be of high quality with no evidence of secondary porosity. As expected for samples of this high permeability, the threshold pressures are very low and all of the samples have low residual vacuum saturations.

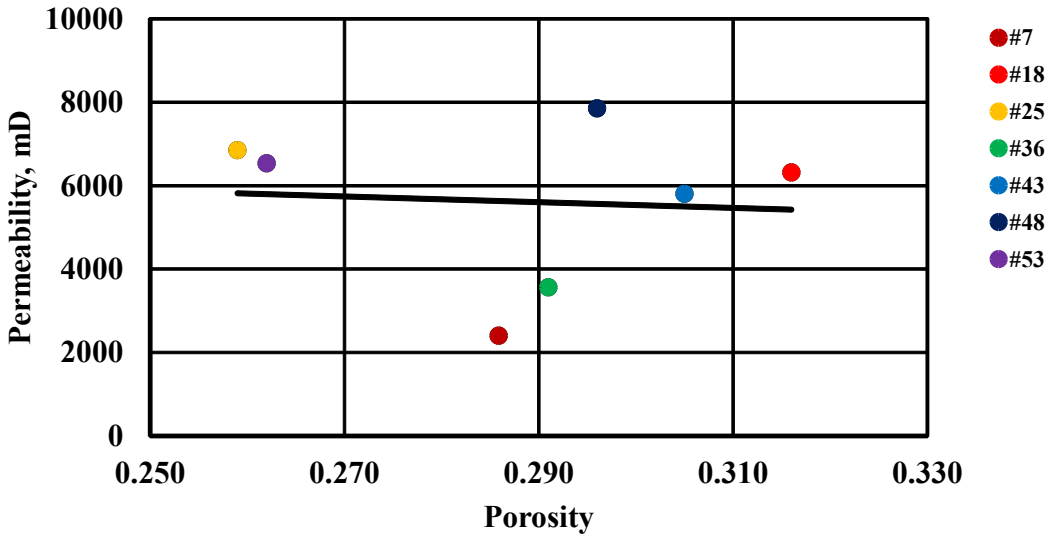

Figure 1. Permeability-Porosity Cross Plot for the MICP Data

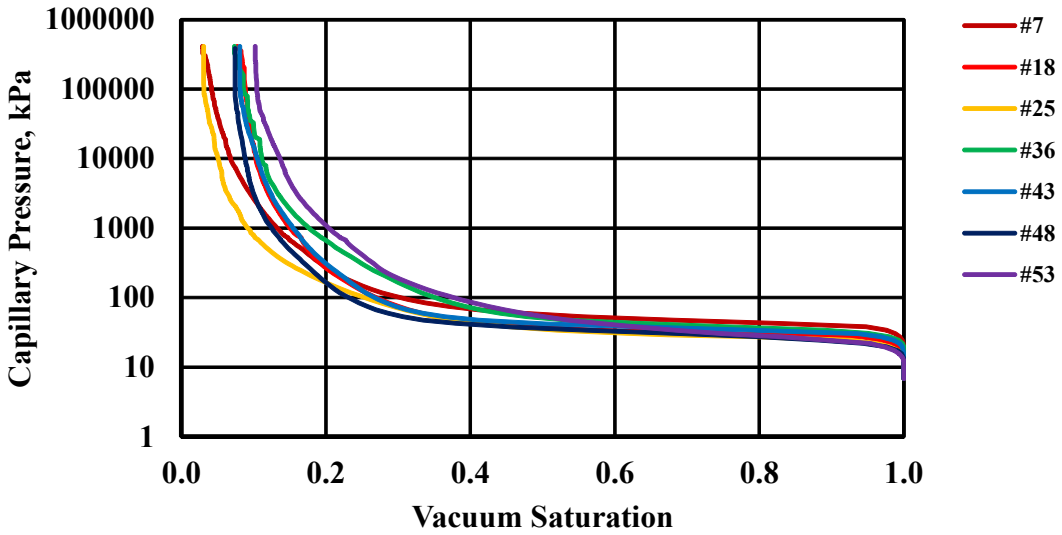

Figure 2. The Mercury Injection Capillary Pressure Curves

The SM permeability is determined by finding the maximum value of the expression

$$k_{SM} = 2.517 \times 10^6 \left(\frac{S_{Hg}\,\phi}{P_c} \right)^{1.691} \qquad (1)$$

Here S_{Hg} is the fractional mercury saturation, ϕ is porosity (decimal), and P_c is the capillary pressure in kPa. k_{SM} has units of mD. Figure 3 shows a cross plot of the SM permeabilities with the measured permeabilities. The SM values are seen to be consistently lower than the experimental values. The maximum error is 84% and the mean error is -67%. This analysis used the conventional values of the correlation parameters (2.517×10^6 and 1.691) in the prediction equation. The systematic trend in the data suggests that much better prediction could be made using different parameters. The calculated values for the SM permeabilities were very similar to those provided by the service laboratory; they used slightly different values of interfacial tension and contact angle (0.485 N/m and 130°) which explains the small differences. The RLAM method is based on assuming that

the sample can be modelling using the simple Representative Elemental Volume illustrated in Figure 4. This element consists of a single tortuous tube, and the permeability is predicted using the equation

$$k_{RLAM} = \frac{\phi\,\delta^2}{32\,\tau^2} \qquad (2)$$

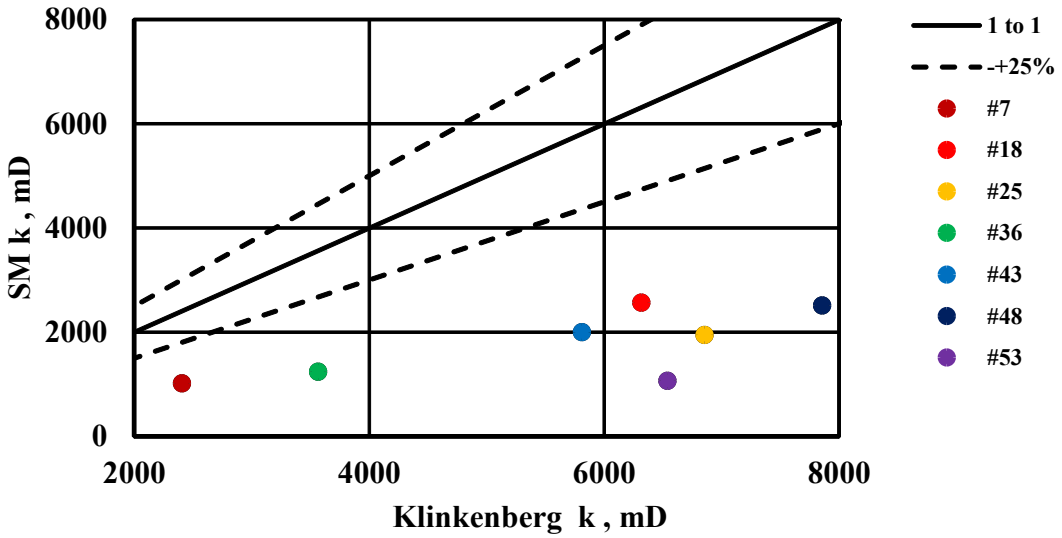

Figure 3. A Comparison between the Permeabilities Predicted by the Swanson Method and the Experimental Values

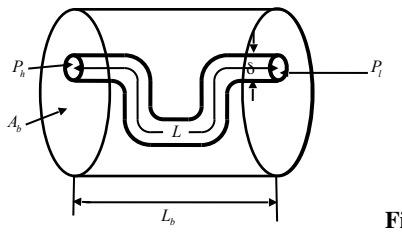

Figure 4. The Representative Elemental Volume

The representative pore diameter is found using a method based on the Purcell equation

$$\delta^2 = (4\,\sigma cos\theta)^2 \int_0^1 \frac{dS_v}{(P_c)^2} \qquad (3)$$

If σ has units of N/m and the capillary pressure has units of Pa; the units for the diameter will then be m, which would be converted to μm before use in Equation 1. In order to apply the RLAM, the formation factors based on electrical properties are needed. Then the tortuosity is found using the following formation factor equation:

Here δ is a representative pore diameter and τ is the tortuosity. If the pore diameter is expressed in μm, then k_{RLAM} will have units of mD.

$$F = \frac{\tau^2}{\phi} \qquad (4)$$

Combining these equations

$$k_{RLAM} = \frac{(\sigma cos\theta)^2}{2\,F} \int \frac{dS_v}{(P_c)^2} \qquad (5)$$

Unfortunately, electrical properties were not available for the MICP samples. However, electrical properties were available for a separate suite of samples taken from the same reservoir and similar, but not exactly the same, depths. Table 2 contains the data for these samples. Figure 5 shows the cross plot of formation factor versus the porosity plus the regression line given by the equation

$$F = \frac{0.85}{\phi^{1.755}} \qquad (6)$$

The regression coefficient for this equation is $R^2 = 0.80$.

Table 2. Data for the Samples used to Determine the Formation Factor Parameters

Sample Identification	Porosity	Formation Factor
N/A	0.262	9.22
N/A	0.272	8.20
3	0.280	7.72
28	0.282	7.37
4	0.283	8.05
N/A	0.286	7.77
30	0.288	7.48
N/A	0.291	7.97
N/A	0.292	7.24
N/A	0.296	7.19
12	0.298	6.98
13	0.301	7.07

Using Equation 5 and the correlation given in Equation 6, the permeabilities were calculated. The results are shown in Figure 6. Three of the predictions are almost exact. The maximum error is 33% and the mean error is -12% which is a significant improvement over the SM results. It is important to note that this method does not use any fitting parameters – it is based strictly on the model assumptions.

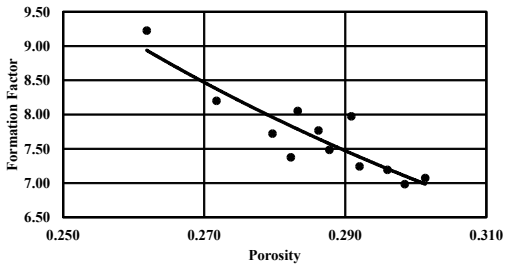

Figure 5. The Formation Factor versus Porosity Cross Plot

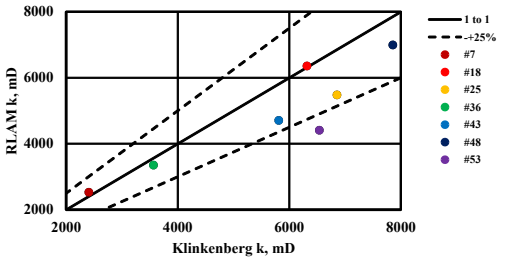

Figure 6. A Comparison between the Permeabilities Predicted by the Ruth-Lindsay-Allen Method and the Experimental Value

3 Relative Permeability Validation

The data set included steady-state relative permeability (SSRP). All SSRP experiments were performed on composite cores of reservoir rock material. The composites contained four individual plugs which were arranged with decreasing permeability from inlet to outlet. Initial water saturation was established by porous plate desaturation for all samples. Ageing was performed over two weeks with live oil at reservoir conditions. Flooding was performed vertically, at reservoir conditions, with injection at the bottom. The stacked cores were approximately 36 cm in length. Experiments were conducted at a temperature of 73 oC and a pore pressure of 270 MPa. Typical water flow rates (those for Sample #7) were 10.80, 32.4, 82.8, 144.0, 234.0, 295.2, 334.8, 352.8, and 360.0 ml/hr and the corresponding oil flow rates were 349.2, 327.6, 277.2, 216.0, 126.0, 64.8, 25.2, 7.2, 0.0 ml/hr. For each of these stacks, one of the samples was a companion sample for one of the MICP samples. In the study described below, the MICP data for the companion sample was assumed to be representative of the entire stack. Three different models were used to predict the SSRP results: the Gates and Tempelaar-Lietz method (GT-LM) [3]; the Burdine method (BM) [4]; and a modified Burdine method (MBM). All of these methods depend on integrating the capillary pressure curve over sub-ranges of the total saturation range in order to obtain wetting component and non-wetting component relative permeabilities. The common difficulty faced by all these methods is that they cannot account for irreducible saturations – the mercury curves start at a vacuum saturation of 1.0 and end at a

vacuum saturation much lower than the wetting component saturation of a typical oil-water experiment. For this reason, only the shapes of the curves were studied – the curves were normalized, the saturations with the total saturation change and the relative permeabilities with their end-points. The details of the methods will be described only for Sample #7. All the other samples behaved in a similar manner. The shapes of the relative permeability curves suggest the samples are moderately oil wet. However, for the purposes of this study it is assumed that water preferentially enters the tubes with smaller diameters. The basic equation used for all the methods is Purcell's original formulation [5] which is written as

$$k_{rw} = \frac{\int_{S_{wr}}^{S_w} \frac{dS_w}{\tau P_c^2}}{\int_{S_{wr}}^{1} \frac{dS_w}{\tau P_c^2}} \quad \text{and} \quad k_{rnw} = \frac{\int_{S_w}^{1} \frac{dS_w}{\tau P_c^2}}{\int_{S_{wr}}^{1} \frac{dS_w}{\tau P_c^2}} \qquad (7)$$

Here the tortuosity τ must be estimated as a function of saturation. The simplest estimate is that tortuosity is a constant. This assumption leads to the GT-LM.

$$k_{rwGLM} = \frac{\int_{S_{wr}}^{S_w} \frac{dS_w}{P_c^2}}{\int_{S_{wr}}^{1} \frac{dS_w}{P_c^2}} \quad \text{and} \quad k_{rnwGLM} = \frac{\int_{S_w}^{1} \frac{dS_w}{P_c^2}}{\int_{S_{wr}}^{1} \frac{dS_w}{P_c^2}} \qquad (8)$$

Figure 7 shows the result of applying the GT-LM to the data for Sample #7. Whereas the predicted wetting component relative permeability curves are reasonable, the non-wetting component curves are in complete disagreement with the experimental data. This is not surprising because for this model the two relative permeabilities must always sum to 1.

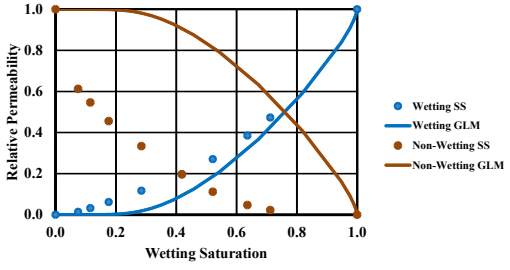

Figure 7. The Normalized Steady State Relative Permeability Curves Compared with the GL-TM Predictions for Sample #7

Burdine assumed that the tortuosity varied in a very specific way with the saturation and arrived at the equations

$$k_{rwBM} = \left(\frac{S_w - S_{wr}}{1 - S_{wr}}\right)^2 \frac{\int_{S_{wr}}^{S_w} \frac{dS_w}{P_c^2}}{\int_{S_{wr}}^{1} \frac{dS_w}{P_c^2}} \quad \text{and} \quad k_{rnwBM} = \left(\frac{S_{nw} - S_{nwr}}{1 - S_{wr} - S_{nwr}}\right)^2 \frac{\int_{S_w}^{1} \frac{dS_w}{P_c^2}}{\int_{S_{wr}}^{1} \frac{dS_w}{P_c^2}} \qquad (9)$$

Figure 8 shows the results for the BM. Here the non-wetting component relative permeability is much better predicted but the wetting component relative permeability is much more poorly predicted. The BM was modified by allowing the exponent on the saturation term to vary. For the non-wetting component, the best value for the exponent was found to be 3; the best value for the wetting component was found to be 0. (The exponent characterizes the manner in which the tortuosity varies with the saturation.) These values were used to calculate the results in Figure 9. The results for the remaining six samples are shown in Figure 10. Visually, the agreement for the non-wetting curves are quite good. This is remarkable given the fact that water is implicitly assumed as the wetting phase (invades the smaller pores) whereas the curves are more characteristic of oil wet samples according to Craig's Rules of Thumb [6]. The difference between the experimental values and the predicted values of the relative permeabilities range from 0.02 to 0.13 with a mean of 0.067. Agreement for the wetting component curves do not appear to be quite as good but are reasonable considering this method is identical to the GL-TM which does not use any correlation parameters. The actual differences for the wetting curves are similar to those for the non-wetting curves, ranging from 0.03 to 0.10 with a mean of 0.062.

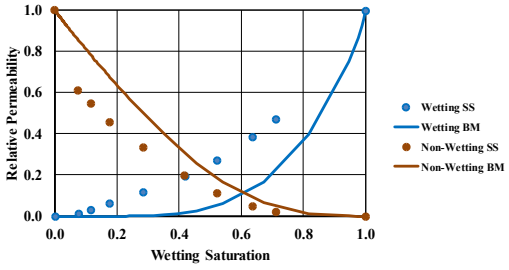

Figure 8. The Normalized Steady State Relative Permeability Curves Compared with the BM Predictions for Sample #7

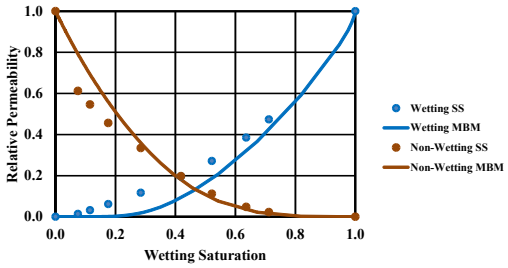

Figure 9. The Normalized Steady State Relative Permeability Curves Compared with the MBM Predictions

4 A Revised Experimental Program

The results presented above were obtained using an existing data set. To optimize this protocol, it is necessary that both electrical testing to determine formation factor and mercury injection capillary pressure be determined for samples that represent each unique feature in the well. The RLAM should then be used to determine if the results are consistent. Two further ideas are worth pursuing. Firstly, electrical tortuosity and diffusive tortuosity are widely accepted to be analogous. Yet diffusion tests are rarely done as part of a core analysis program. Experimental procedures that use diffusion tests should be developed. Secondly, resistivity index experiments should contain information on how pore networks are connected. The connection between relative permeability and resistivity index has never been fully explored. It would be useful for resistivity index experiments to be routinely performed on samples that are to be tested for relative permeability.

5 Conclusions

Using a very simple model for the porous media, this study shows that porosity, permeability, electrical properties, and mercury injection capillary pressure all show mutually consistent behaviors that is, the measured permeability and the permeability calculated using the other properties in the simple model are in acceptable agreement. Furthermore, the analysis was extended to give reasonable predictions of the shapes of steady-state relative permeability curves. Although these agreements could be purely coincidental, the authors contest that the agreement can be taken to mean that the core analysis results are valid.

This work was supported by an Engage Grant from the Natural Sciences and Engineering Research Council of Canada. The authors thank Equinor for providing the data used in this study.

References

1. Swanson, B.F.,"A Simple Correlation Between Permeabilities and Mercury Injection Capillary Pressures", Paper SPE-8234, Journal of Petroleum Technology, (1981), 33, 12, 2498-2504.
2. Ruth, D.W., Lindsay, C., and Allen, M., "Combining Electrical Measurements and Mercury Porosimetry to Predict Permeability", Petrophysics, (2013), 54, 6, 531-537.
3. Gates, J.I. and Tempelaar-Lietz, W. "Relative Permeabilities of California Core by the Capillary-Pressure Method", API Drilling and Production Practice, (1950), 285-302.
4. Burdine, N.T., "Relative Permeability Calculations from Pore Size Distribution Data", AIME Transactions, (1953), 198, 71-78, TP3519.
5. Purcell, W.R., "Capillary Pressures – Their Measurement using Mercury and the Calculation of Permeability Therefrom", Paper SPE-94049-G, Journal of Petroleum Technology, (1949), 1, 2, 39-48, (AIME Transactions, 186).
6. Craig, F. F. Jr., "The Reservoir Engineering Aspects of Waterflooding", SPE, (1977).

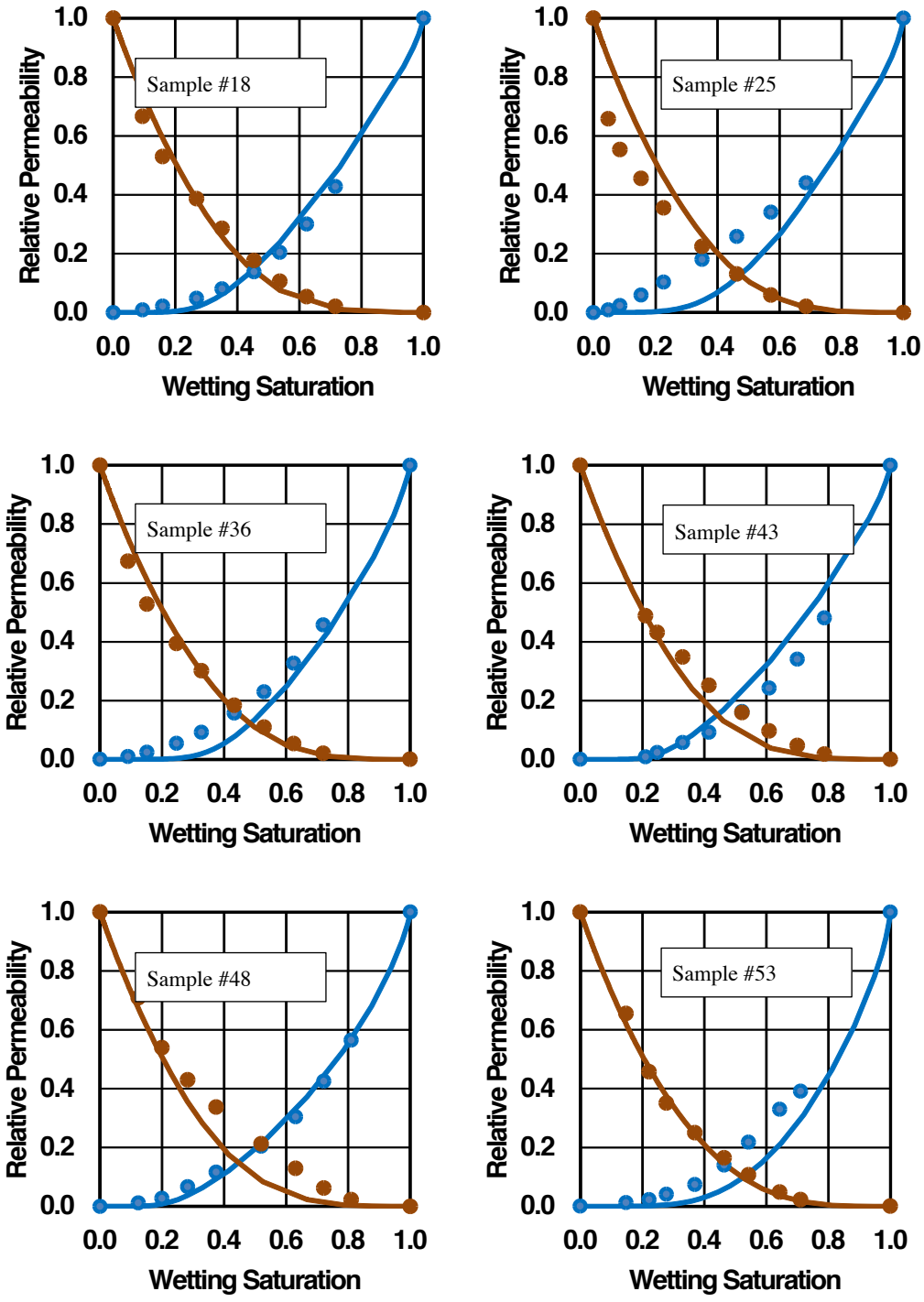

Figure 10. Comparisons for the Normalized Steady State Relative Permeability Curves